J. Phys. B: At. Mol. Opt. Phys. 26 (1993) 4537–4551. Printed in the UK

Single-centred calculations of excitation and electron removal in intermediate energy proton–hydrogen collisions

A L Ford, J F Reading and K A Hall

Center for Theoretical Physics, Physics Department, Texas A&M University, College Station, TX 77843, USA

Received 8 July 1993, in final form 28 September 1993

Abstract. Single-centred expansion coupled states calculations are performed with basis sets large enough to achieve convergence. The particular collision system studied is p + H(1s) at energies of 15 keV and above. The results obtained establish the validity of this method for calculating excitation and electron removal cross sections even in situations where charge transfer is large. Cross sections for $1s \rightarrow 2l'$, $3l'$ and $4l'$ excitation and for electron removal are presented and compared to experiment and to other theoretical calculations.

1. Introduction

Coupled states calculations have been widely used to calculate excitation, ionization, and charge transfer cross sections in ion–atom collisions (for a recent review, see Fritsch and Lin 1991). In symmetric or nearly symmetric collisions at energies near velocity matching between the projectile velocity and the velocity of the active target electron, charge transfer cross sections are large and this poses calculational difficulties because it introduces a two-centred character into the problem. The traditional method for dealing with charge transfer is to use a two-centred basis expansion, with some orbitals centred on the target nucleus and some on the projectile. Such calculations are very time consuming and it is difficult to achieve convergence in the basis size. There is also the problem of linear dependence in the basis; the two sets of orbitals on the two centres are not orthogonal to each other when the projectile and target are not far apart.

There have been a number of attempts at circumventing the problem of two-centred expansions. Our own group developed the 'one and a half centred expansion' (OHCE) approach (Reading *et al* 1981). In this method flux loss from the target region due to charge transfer is represented by including projectile-centred functions in the expansion of the wavefunction but the expansion coefficients for these basis functions have prechosen time dependence. The method works because a large target-centred basis can adequately represent projectile orbitals when the projectile and target are close together, and this is where the interaction is large and transitions occur. As the projectile and target separate the projectile-centred functions allow the electron to leave the target region in a bound state of the projectile. With a single projectile-centred function (the 1s) we applied this method to $p + H$ collisions (Reading *et al* 1981), to $p + He^+$ and $He^{2+} + H$ collisions (Reading *et al* 1982) and to $p + Li^{+,2+}$ and $Li^{2+,3+} + H(1s)$ collisions (Ford *et al* 1982), and showed that it allowed for accurate calculation of excitation, ionization, and charge transfer cross sections. The OHCE retains the computational efficiency of a single-centred expansion (SCE), but does require calculation of two-centred matrix elements. Recently Ermolaev used an asymmetric

0953-4075/93/234537+15$07.50

two-centred expansion to study $p^{\pm} + H$ and other collision systems (Ermolaev 1990a, b). These calculations use a large target-centred basis and a single function (the 1s) centred on the projectile to account for charge transfer.

Several groups have used purely target-centred expansions. Previous SCE calculations for p + H by our group (Fitchard *et al* 1977) and by Bransden *et al* (1979) used only s, p and d orbitals and the results are good only at high energies where charge transfer is small. Very recently Reinhold *et al* (1990) used a large basis (74 states) that included all hydrogen atom bound states up through $n = 5$, so their basis must have had l values at least up through $l = 4$ (g states). They considered excitation by fully stripped ions of charge q from 1 to 26 and excitation from both ground and excited levels of hydrogen ($n = 2, 3$). They also performed CTMC and symmetric eikonal calculations and the symmetric eikonal results for $1s \rightarrow n' = 2$, 3 and 4 excitation are in good agreement with their coupled channels results. Due to lack of states centred on the projectile, they estimated that their coupled channels calculations were appropriate only at energies above 60 keV for p + H(1s).

In the course of preliminary work on calculation of excitation with higher n levels ($n = 2$, 3 and 4) as initial and final states we have reexamined the use of single-centred expansions. Adequate description of all important final and virtual intermediate states in such collisions requires a large basis that includes a number of angular momentum l values. With such large basis sets two-centred or even one and a half centred calculations become impractical. But we have found that if the basis is sufficiently large and includes enough l values then the single-centred expansion can be made to converge even at collision energies where charge transfer is large. For this to happen the target-centred basis must be able to represent all important projectile centred orbitals for all projectile-target separations at which transitions occur. We report on such calculations for $1s \rightarrow n' = 2$, 3 and 4 excitation in p + H(1s) collisions at energies of 15 keV and above. We also examine the cross section summed over continuum pseudostates and interpret this as the total electron removal cross section, the sum of ionization and charge transfer.

The purpose of this paper is twofold. One is to establish the method of very large basis set single-centred expansions. We examine the results for the well studied case of p + H(1s) collisions to show that such calculations can produce cross sections of high accuracy. In subsequent publications we will apply this same method to collisions involving excited hydrogen and to other few-electron collision systems. But the cross sections we report here are also of interest in and of themselves. There is not complete agreement between theory and experiment or between different calculations even for this simple, fundamental system. For this reason we present our results in detail and compare with what previously has been published.

We very briefly summarize the computational procedure in section 2. In section 3 we present our results and compare to experiment and to other calculations. We give a summary and conclusions in section 4.

2. Method

The coupled-states calculations reported here use methods that have been described previously (Fitchard *et al* 1977, Ford *et al* 1977) and so will be only briefly summarized here. The projectile is treated as a classical particle moving on a straight-line constant-velocity path. The projectile thus serves to provide a time-dependent perturbation $V(r, t)$ of the target atom. Transition amplitudes were calculated by a time-development operator

U-matrix approach. This method consists of writing the U matrix which connects the wavefunction at time t_1 to that at t_3 as

$$\underline{\Psi}_I(t_3) = \underline{U}(t_3, t_1)\underline{\Psi}_I(t_1) \approx \exp\left[-\frac{i}{\hbar v}\int_{t_1}^{t_3} \underline{V}_I(t')\,dt'\right]\underline{\Psi}_I(t_1). \tag{1}$$

In this equation we work in the interaction picture. A bar under a wavefunction or operator indicates its matrix in the space of our basis. The transition amplitudes are the elements of the matrix $\underline{U}(t_L, -t_L)$, where t_L is some large time at which the projectile–target interaction is negligible. The $\underline{U}(t_L, -t_L)$ matrix is calculated from a time-ordered product of $\underline{U}(t_i, t_{i-2})$ calculated as in equation (1) for small time steps t_{i-2} to t_i. The integrals in equation (1) are calculated numerically using a grid that has one t-value between t_1 and t_3. The time grid must contain enough points to allow for accurate calculation of the potential matrix elements and also must contain sufficiently small time steps for the first Magnus approximation for each small time interval to be accurate.

Our basis states are matrix eigenvectors of the target (in this case a hydrogen atom) Hamiltonian and are obtained by diagonalizing this Hamiltonian on an underlying basis of the form $\phi_{ilm} = r^l e^{-\lambda_i r} Y_{lm}$, where the λ_i are complex. In the present calculations we used the same set of λ_i and therefore the same number of radial functions, for each l value. The diagonalization of the target Hamiltonian on this basis yields an accurate representation of the low-lying bound states and also produces pseudostates that provide a discrete representation of the ionization continuum. For example, with the basis set we used that has 13 radial functions for each l, in the case of $l = 0$ there are 5 bound states and 8 continuum pseudostates that extend in energy up to 350 eV above the ionization threshold. For $l = 5$ the basis has 3 bound pseudostates and 10 continuum pseudostates extending in energy up to 90 eV above the ionization threshold.

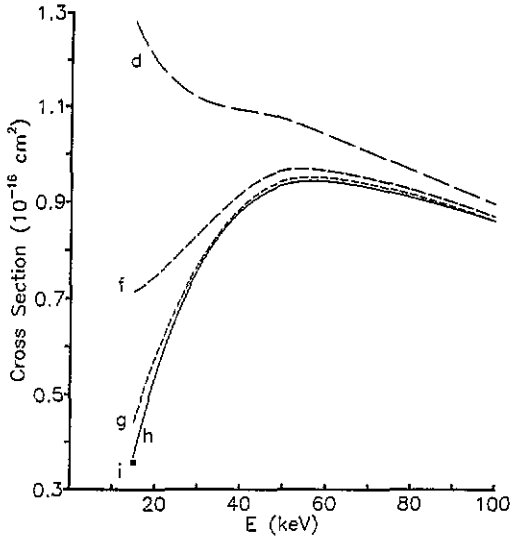

Figure 1. Angular momentum convergence of the 1s → $n' = 2$ excitation cross section. The curves are labelled with the maximum l used in the basis. One point at 15 keV for $l_{max} = 6$ (i states) is shown. Excellent convergence is seen above 15 keV if up through $l = 5$ (h states) are included in the basis.

3. Results

The single-centred expansion method is based on the ability of the target-centred basis to represent projectile-centred orbitals for a sufficient range of projectile–target separations. Figure 1 shows the convergence in l_{max}, the maximum value of l included in the basis, for the $1s \rightarrow n' = 2$ cross section. At sufficiently high energies the cross sections merge with the first Born and in this limit only the l values of the initial and final states are needed. The particular cross section shown here approaches the Born from below and is within 5% at 300 keV. For this symmetric collision system the capture cross section does not pass through a maximum as the collision energy is lowered but instead monotonically increases until a constant value is reached at low energies. Therefore, as the energy is lowered and the capture cross section increases, more l values are needed to achieve convergence. For collision energies 30 keV and above comparison of $l_{max} = 4$ and $l_{max} = 5$ calculations indicates l-convergence of about 1% when $l_{max} = 5$ (h states). The l-convergence starts to break down at 15 keV, where calculations with $l_{max} = 6$ (i states) differ from $l_{max} = 5$ results by about 5%. Similar l-convergence is found for all $1s \rightarrow n'l'$ transitions for $n' = 2$, 3 and 4.

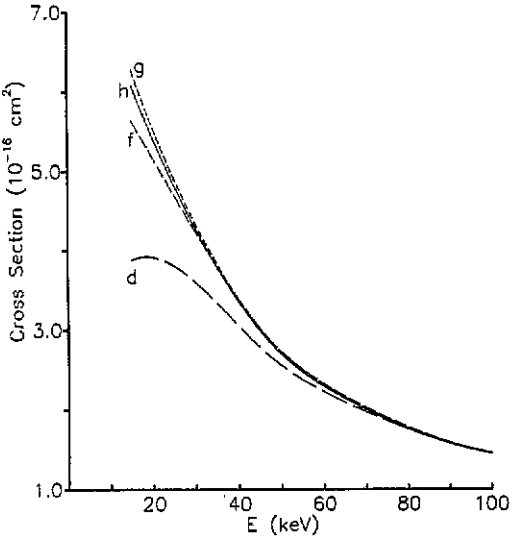

Figure 2. Angular momentum convergence of the H(1s) electron removal cross section. The curves are labelled with the maximum l used in the basis. Excellent convergence is seen above 15 keV if up through $l = 5$ (h states) are included in the basis.

Figure 2 shows the l-convergence for the H(1s) electron removal cross section. The single-centred calculation does not calculate the separate ionization and capture components of this cross section, just their sum. At high energies the electron removal cross section is dominated by ionization and at the lower energies it is dominated by electron capture. These two cross sections are equal at around 45 keV. In Figure 2 the first Born ionization cross section calculated with our pseudostate basis for those l values not included in the set of coupled states, up through $l = 6$, has been added to each cross section. This accelerates the convergence in l_{max} for the higher energies where the ionization dominates. The convergence in l_{max} is similar to that discussed above for excitation.

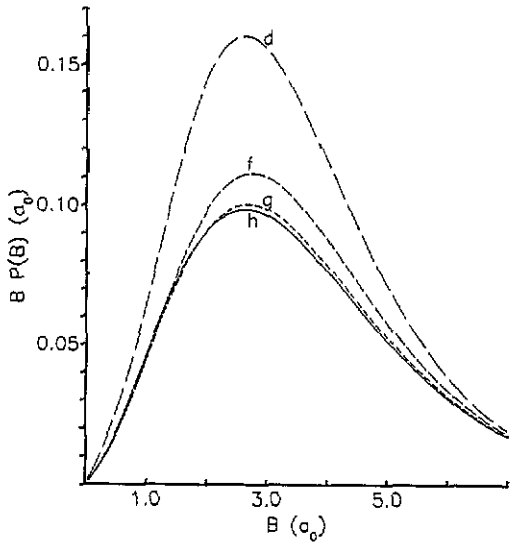

Figure 3. Angular momentum convergence of the impact parameter dependent probability $P(B)$ for $1s \rightarrow n' = 2$ excitation at $E = 30$ keV. The probability $P(B)$ times impact parameter B is plotted versus B, where B is given in units of the Bohr radius a_0. The cross section is therefore 2π times the area under the curve. The curves are labelled with the maximum l used in the basis.

The l-convergence has also been examined at the impact parameter level. Figure 3 shows the angular momentum convergence of the impact parameter dependent probability $P(B)$ for $1s \rightarrow n' = 2$ excitation at a collision energy of $E = 30$ keV. The convergence shown in the figure is quite good, with little difference seen between $l_{max} = 4$ (g states) and $l_{max} = 5$ (h states) calculations. The convergence at the $P(B)$ level is slightly poorer than for the cross section. Going from $l_{max} = 4$ to $l_{max} = 5$ increases $P(B)$ by about 5% for impact parameter $B < 1\ a_0$ and decreases $P(B)$ by about 2.5% around $B = 4\ a_0$. Therefore there is some cancellation and the cross section changes by only 1.2%. The convergence is somewhat less good for the individual $1s \rightarrow 2s$ and $1s \rightarrow 2p$ excitation probabilities, particularly at small impact parameter. For the $1s \rightarrow 2s$ transition, $P(B)$ around $B = 0.1\ a_0$ increases by 10% when l_{max} is increased from 4 to 5 and for $1s \rightarrow 2p$ it decreases by 22%. These small impact parameters contribute little to the cross sections and the cross sections change by only 1%. The difficulty in obtaining convergence at small B is presumably due to the large interaction provided by the projectile when it makes a close approach to the target.

Figure 4 shows in a similar way the l-convergence for the probability for H(1s) electron removal at $E = 30$ keV. The convergence at $l_{max} = 5$ is again quite good. The convergence becomes poorer as B increases. At $B = 5.4\ a_0$, for example, $P(B)$ increases by 56%, 14% and 2%, respectively, as l_{max} is increased from 2 to 3, 3 to 4 and 4 to 5. At $B = 7.6\ a_0$ the corresponding increases in $P(B)$ are 71%, 22% and 5%. But, as figure 4 shows, impact parameters larger than $5\ a_0$ make only a small contribution to the cross section. The problem in obtaining convergence at large impact parameters must reflect the difficulty of expanding projectile-centred orbitals in our target-centred basis when the projectile and target are far apart. This convergence problem at large B is not present in the excitation probabilities because at large B the projectile interaction is weak and the ionization channels do not couple appreciably to the excitation.

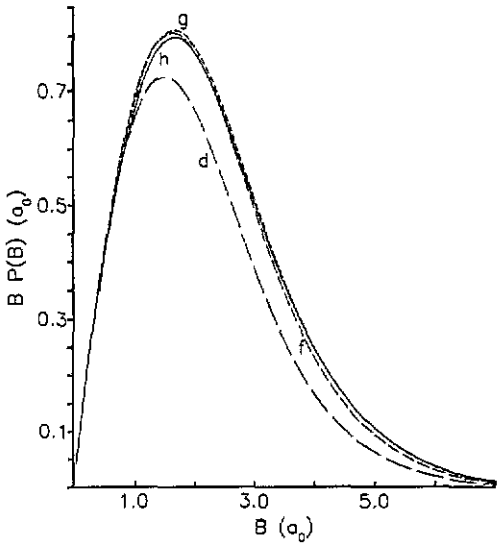

Figure 4. *Angular momentum convergence of the impact parameter dependent probability $P(B)$* for H(1s) electon removal at $E = 30$ keV. The probability $P(B)$ times impact parameter B is plotted against B, where B is given in units of the Bohr radius a_0. The cross section is therefore 2π times the area under the curve. The curves are labelled with the maximum l used in the basis.

Table 1. Convergence in l_{max} of the H(1s) electron removal cross section. All cross sections are given in units of 10^{-16} cm^2. For each $l > l_{max}$ the first Born ionization cross section calculated with our basis functions is given and included in the total. For each l value the number in parentheses is the per cent that l contributes to the total. The number in parentheses after each *total cross section is the per cent difference from the previous l_{max} result.*

Partial wave	$l_{max} = 2$	$l_{max} = 3$	$l_{max} = 4$	$l_{max} = 5$
$E = 30$ keV				
$l = 0$	0.691 (19%)	0.502 (12%)	0.355 (8.2%)	0.278 (6.5%)
$l = 1$	1.335 (37%)	1.043 (25%)	0.714 (16%)	0.540 (13%)
$l = 2$	1.377 (38%)	1.417 (33%)	1.118 (26%)	0.860 (20%)
$l = 3$	0.138 (3.8%)	1.216 (29%)	1.152 (27%)	0.976 (23%)
$l = 4$	0.045 (1.2%)	0.045 (1.1%)	0.985 (23%)	0.897 (21%)
$l = 5$	0.017 (0.5%)	0.017 (0.4%)	0.017 (0.4%)	0.734 (17%)
$l = 6$	0.007 (0.2%)	0.007 (0.2%)	0.007 (0.2%)	0.007 (0.2%)
Total	3.610	4.247 (+18%)	4.348 (+2.4%)	4.292 (−1.3%)
$E = 150$ keV				
$l = 0$	0.0984 (9.7%)	0.0945 (9.3%)	0.0946 (9.4%)	
$l = 1$	0.5114 (51%)	0.4875 (48%)	0.4838 (48%)	
$l = 2$	0.3037 (30%)	0.2803 (28%)	0.2705 (27%)	
$l = 3$	0.0613 (6.1%)	0.1132 (11%)	0.1059 (10%)	
$l = 4$	0.0234 (2.3%)	0.0234 (2.3%)	0.0416 (4.1%)	
$l = 5$	0.0095 (0.9%)	0.0095 (0.9%)	0.0095 (0.9%)	
$l = 6$	0.0039 (0.4%)	0.0039 (0.4%)	0.0039 (0.4%)	
Total	1.0116	1.0123 (+0.07%)	1.0098 (−0.25%)	

An interesting feature of the electron removal cross sections as calculated here is that the total cross section, summed over l of the final state, is much more stable than the individual

l partial wave cross sections. This is illustrated in table 1 at a low (30 keV) and a high (150 keV) energy. For example, at 30 keV in the $l_{max} = 5$ calculation the $l = 5$ partial wave cross section adds 17% but the other partial wave contributions adjust to make the total cross section change by less than 2% compared to the $l_{max} = 4$ result. At 150 keV the convergence for each partial wave is much better than at 30 keV, but the total is still much better converged than each partial wave cross section. At 150 keV the first Born ionization cross section is 0.928×10^{-16} cm^2; our coupled channels cross section is 9% above the Born. As the energy is increased our cross section approaches the first Born from above and comes to within 5% of the Born at around 200 keV.

There are other aspects to the convergence of our calculations in addition to the convergence in the maximum angular momentum in the basis. One is the number of time integration points. The bulk of the calculations was done with 181 points, with selected calculations done with 121 or 341 points to test the convergence. With 181 points the first Born cross sections are converged to within 0.5% or less. In the coupled-channels calculations the time integration mesh also determines the size of the time intervals on which the first Magnus approximation is used in calculating the time-development U-matrix. In these calculations all cross sections considered here are converged to within 5% at 15 keV and 30 keV and to within 1% at higher energies. We must also consider the convergence in the number of radial functions used for each l. The results reported here were done with 13 radial functions for each l. This leads to 78 coupled channels for $l_{max} = 2$, 130 for $l_{max} = 3$, 195 for $l_{max} = 4$, 273 for $l_{max} = 5$ and 364 for $l_{max} = 6$. To test the convergence we did selected calculations with 9 and with 17 radial functions. These tests indicate that the 13-state calculations are converged to within 5% at 15 keV and to within 1.5% or better at 30 keV and higher energies. Considering all sources of inaccuracy we estimate that all cross sections reported here are accurate to within 3% at all energies except 15 keV, where the error could be as large as 8 to 10%.

As the above discussion has indicated, the convergence in l_{max} and in the time integration mesh becomes less rapid as the collision energy is lowered. We attempted calculations at 5 keV but were unable to achieve satisfactory convergence in either l_{max} or in the time integration mesh. For this collision system, the single-centred expansion as we have implemented it appears to be computationally impractical at energies below 15 keV.

Table 2. The $n' = 2$ excitation cross sections (in units of 10^{-17} cm^2).

	1s → 2s			1s → 2p		
E (keV)	Present	Sh[a]	POHC[b]	Present	Sh[a]	POHC[b]
15	0.950	0.88	0.93	2.58	2.46	2.4
30	1.80		1.6	5.78		6.3
45	1.76			7.41		
60	1.52	1.32	1.6	7.92	7.29	8.4
80	1.24			7.89		
100	1.02		0.98	7.62		7.8
125	0.829			7.13		
150	0.694			6.64		
200	0.519	0.49		5.79	5.55	

[a] Two-centred Sturmian basis calculations of Shakeshaft (1978).
[b] One-and-a-half-centred calculations of Reading *et al* (1981).

3.1. Excitation

Our results for the $1s \rightarrow n' = 2$ excitation cross section are compared to the experimental data of Park *et al* (1976) in figure 5. The Park *et al* data were originally normalized to a Born cross section of 6.637×10^{-17} cm^2 at 200 keV. Since our calculations show some deviation from first Born at this energy we have normalized the Park *et al* data to agree with our coupled states cross section of 6.312×10^{-17} cm^2. This involves multiplying the numbers given in the Park *et al* (1976) paper by a factor of 0.951. The agreement between theory and experiment shown in figure 5 is quite good. Our calculations are somewhat below experiment at the cross section peak but otherwise fall within the experimental error bars. There have been numerous other coupled states calculations of this cross section but none, except for our earlier OHCE calculation (Reading *et al* 1981), are in as good agreement with experiment over the entire 15 keV to 200 keV energy range as is the present calculation. The asymmetric two-centred calculations of Ermolaev (1990a) extend down only to 30 keV and are above the data below 40 keV. The two-centred Sturmian basis calculations of Shakeshaft (1978) in general are in excellent agreement with the experimental data except at 60 keV, where the calculations show a dip not seen in the data. The two-centred calculations of Fritsch and Lin (1983) extend only up to 75 keV and at this energy have fallen below the data. The single-centred AO calculations of Reinhold *et al* (1990), that used 74 basis functions, are included in figure 5 and are in good agreement with our results. Their results are actually closer to the experiment at the cross section peak, but the lowest energy for which they reported results is 40 keV. The individual $1s \rightarrow 2s$ and $1s \rightarrow 2p$ cross sections are given in table 2 and are compared there to the calculations of Shakeshaft and to our previous POHCE one-and-a-half-centred calculations. The agreement is good.

Table 3. Approach of the coupled-channels (CC) $n' = 2$ excitation cross sections to first Born. (Cross sections in units of 10^{-17} cm^2.)

	$1s \rightarrow 2s$			$1s \rightarrow 2p$			$1s \rightarrow n' = 2$		
E (keV)	CC	Born	CC/Born	CC	Born	CC/Born	CC	Born	CC/Born
100	1.020	0.903	1.13	7.62	9.58	0.80	8.64	10.49	0.82
150	0.694	0.617	1.12	6.64	7.61	0.87	7.34	8.23	0.89
200	0.519	0.469	1.11	5.79	6.37	0.91	6.31	6.84	0.92
250	0.413	0.378	1.09	5.13	5.51	0.93	5.54	5.89	0.94
300	0.342	0.317	1.08	4.61	4.89	0.94	4.95	5.20	0.95
400	0.254	0.239	1.06	3.85	3.99	0.96	4.10	4.23	0.97
500	0.202	0.192	1.05	3.31	3.41	0.97	3.52	3.60	0.98
750	0.133	0.129	1.03	2.49	2.53	0.98	2.62	2.66	0.98
1000	0.0991	0.0968	1.02	2.02	2.04	0.99	2.12	2.14	0.99

At high collision velocities, or if we set the projectile charge Z_p to some artificial and unphysical small value, such as $Z_p = 1 \times 10^{-5}$, our coupled states calculation results become identical to the first Born approximation. Our pseudostate basis contains sufficiently accurate representations of the exact 1s, 2s and 2p states and our numerical methods are sufficiently accurate that we reproduce analytical first Born results calculated with the exact wavefunctions to well within 1%. It is of interest to look at the approach of the coupled states cross sections (with the full potential strength) to first Born as the collision energy is increased. This comparison is made in table 3. It is seen that the $1s \rightarrow 2s$ cross section approaches the Born from above and the $1s \rightarrow 2p$ from below. The approach to the Born

is also rather slow, with 5% corrections to first Born remaining up to 500 keV for $1s \rightarrow 2s$ and up to 400 keV for $1s \rightarrow 2p$.

Our results for $1s \rightarrow n' = 3$ excitation are presented and compared to experiment in figure 6. The experimental data of Park *et al* were renormalized as discussed above by multiplying by a factor of 0.951. The agreement of our calculations with the data is good except at the cross section peak where our results are below the experimental data. The asymmetric two-centred calculations of Ermolaev (1990a, 1991) agree well with our calculations at 75 keV and are closer to the data near the cross section peak. However, they extend down only to 30 keV. The single-centred calculations of Reinhold *et al* (1990) agree closely with our results, becoming slightly higher and therefore closer to the experiment at their two lowest energies of 40 and 60 keV. The Shakeshaft (1978) calculation (not shown in the figure) again has structure (a dip around 90 keV) not seen in the experimental data.

Table 4. The $n' = 3$ excitation cross sections (in units of 10^{-18} cm^2). The rows in parentheses labelled Em are from Ermolaev (1991), those labelled Sh are from Shakeshaft (1978) and those labelled POHCE are from Reading *et al* (1981). The experimental Balmer alpha emission cross sections are from Donnelly *et al* (1991).

						Balmer alpha emission σ_{em}	
E (keV)		3s	3p	3d	Total $n' = 3$	Theory	Expt
15		1.63	4.12	1.65	7.40	3.77	5.85 ± 0.59
	(Sh)	(1.8)	(4.7)	(2.1)	(8.6)	(4.5)	
	(POHCE)	(1.7)	(4.0)	(2.1)	(7.8)	(4.3)	
30		3.89	8.87	3.20	15.97	8.14	17.34 ± 1.21
	(Em)	(1.60)	(13.00)	(4.22)	(18.82)	(7.35)	
	(POHCE)	(3.5)	(10)	(4.2)	(18)	(8.9)	
45		3.96	11.97	3.30	19.23	8.67	
60		3.43	13.13	2.87	19.43	7.85	15.58 ± 0.62
	(Em)	(2.10)	(15.35)	(3.59)	(21.04)	(7.50)	
	(Sh)	(3.8)	(13.20)	(3.9)	(20.9)	(9.3)	
	(POHCE)	(3.3)	(14)	(3.4)	(21)	(8.4)	
80		2.75	13.29	2.28	18.32	6.60	11.98 ± 0.72
100		2.24	12.92	1.86	17.02	5.62	10.38 ± 0.57
	(Em)	(1.43)	(13.68)	(2.02)	(17.13)	(5.06)	
	(POHCE)	(2.1)	(13)	(2.1)	(17)	(5.7)	
125		1.79	12.14	1.47	15.41	4.69	
150		1.48	11.32	1.21	14.01	4.03	
200		1.09	9.86	0.872	11.82	3.12	
	(Em)	(0.69)	(10.26)	(0.88)	(11.83)	(2.78)	
	(Sh)	(1.1)	(9.9)	(0.94)	(11.94)	(3.2)	

Our cross sections for the individual $1s \rightarrow 3s$, $1s \rightarrow 3p$, and $1s \rightarrow 3d$ transitions are given in table 4 and compared to our earlier POHCE calculations (Reading *et al* 1981), to the two-centred sturmian basis calculations of Shakeshaft (1978) and to the asymmetric two-centred expansion calculations of Ermolaev (1991). The agreement among the various calculations is much poorer than for 2s and 2p excitation. Our calculation for $1s \rightarrow 3d$ is well below both the POHCE and Shakeshaft results. This is not surprising since the basis sets used in each of these latter calculations included only up through d sates. It is reasonable to expect that for 3d excitation coupling to f states is important and that as a consequence

the present calculations are more accurate. Even though the Ermolaev calculation gives a total $n' = 3$ excitation cross section in reasonable agreement with our calculation the two calculations differ substantially in the individual $3l'$ cross sections. In particular, Ermolaev's $1s \rightarrow 3s$ cross section is substantially below ours at all energies. At 200 keV the first Born $1s \rightarrow 3s$ cross section is 0.932×10^{-18} cm^2; it is difficult to understand how Ermolaev's cross section of 0.69×10^{-18} cm^2 could be accurate. In table 5 we show the approach of our coupled-states calculations to the first Born as the collision energy is increased. The $1s \rightarrow 3s$ and $1s \rightarrow 3d$ cross sections slowly approach the Born from above and the $1s \rightarrow 3p$ cross section approaches the Born from below. At 500 keV the $1s \rightarrow 3s$ and $1s \rightarrow 3d$ cross sections are 7% and 10% above the Born.

Table 5. Approach of the coupled-channels (cc) $n' = 3$ excitation cross sections to first Born. (Cross sections in units of 10^{-18} cm^2.)

	$1s \rightarrow 3s$			$1s \rightarrow 3p$		
E (keV)	cc	Born	cc/Born	cc	Born	cc/Born
100	2.24	1.80	1.24	12.9	16.6	0.78
150	1.48	1.23	1.20	11.3	13.1	0.86
200	1.090	0.932	1.17	9.86	10.87	0.91
250	0.858	0.752	1.14	8.72	9.38	0.93
300	0.705	0.630	1.12	7.81	8.29	0.94
400	0.517	0.475	1.09	6.51	6.76	0.96
500	0.408	0.382	1.07	5.59	5.75	0.97
750	0.267	0.256	1.04	4.18	4.25	0.98
1000	0.199	0.192	1.04	3.37	3.41	0.99
	$1s \rightarrow 3d$			$1s \rightarrow n' = 3$		
E (keV)	cc	Born	cc/Born	cc	Born	cc/Born
100	1.86	1.23	1.51	17.0	19.6	0.87
150	1.21	0.870	1.39	14.0	15.2	0.92
200	0.872	0.674	1.29	11.8	12.5	0.94
250	0.676	0.549	1.23	10.3	10.7	0.96
300	0.550	0.465	1.18	9.07	9.39	0.97
400	0.400	0.353	1.13	7.42	7.59	0.98
500	0.314	0.285	1.10	6.31	6.42	0.98
750	0.204	0.193	1.06	4.65	4.70	0.99
1000	0.151	0.145	1.04	3.72	3.75	0.99

There is an unresolved discrepancy between theory and experiment (Donnelly *et al* 1991) for the cross section for Balmer alpha emission from hydrogen atoms excited by protons in the 15 to 100 keV energy region. This emission cross section is given (Ermolaev 1991) by $\sigma_{em} = \sigma(1s \rightarrow 3s) + 0.118\sigma(1s \rightarrow 3p) + \sigma(1s \rightarrow 3d)$, where the $\sigma(1s \rightarrow 3l')$ are the cross sections for excitation by proton impact. The values of σ_{em} calculated from the three different theoretical cross sections are also given in table 4. Even though our cross sections for the different $\sigma(1s \rightarrow 3l')$ excitations differ from those of Ermolaev, the σ_{em} calculated from them do not differ greatly and our results do not remove the large (factor of two) discrepancy between theory and experiment. It is recognized that the experimental results contain a cascade contribution, but this has been estimated (Ermolaev 1991) to be much too small to explain the discrepancy and our calculations do not suggest any serious error in this estimate.

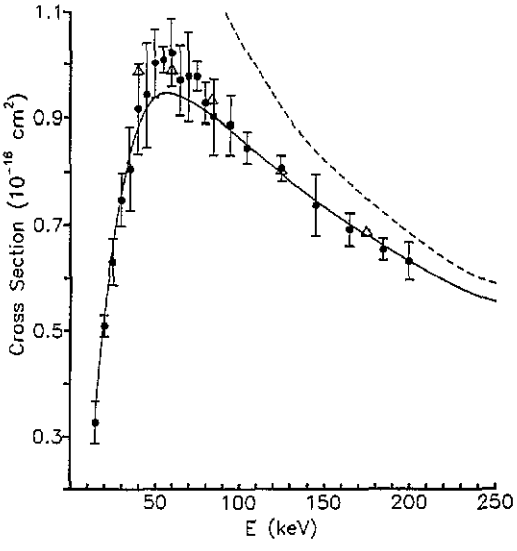

Figure 5. The 1s → $n' = 2$ excitation cross section. The experimental points with error bars are from Park *et al* (1976), renormalized to our calculation at 200 keV. The full curve is the present calculation and the broken curve is the first Born approximation. The open triangles are the single-centred expansion calculation of Reinhold *et al* (1990). Note that the vertical scale is linear.

Table 6. The $n' = 4$ excitation cross sections (in units of 10^{-18} cm^2).

E (keV)	1s → 4s	1s → 4p	1s → 4d	1s → 4f	Total $n' = 4$
30	1.46	2.93	1.44	0.16	5.99
45	1.55	4.07	1.55	0.12	7.29
60	1.35	4.53	1.37	0.077	7.33
80	1.07	4.64	1.10	0.048	6.86
100	0.870	4.54	0.892	0.033	6.34
150	0.570	4.00	0.580	0.016	5.17
200	0.416	3.49	0.416	0.0095	4.33
250	0.326	3.09	0.322	0.0066	3.74
300	0.267	2.77	0.262	0.0050	3.30
400	0.195	2.30	0.190	0.0035	2.69
500	0.154	1.98	0.149	0.0026	2.29
750	0.100	1.47	0.0967	0.0016	1.67
1000	0.0741	1.19	0.0717	0.0011	1.34

Our basis contains excellent representations of the $n' = 4$ levels and the $\sigma(1s \rightarrow 4l')$ cross sections appear to be converged at the few per cent level. In particular, our basis gives first Born cross sections well within 1% of the exact values. Our $\sigma(1s \rightarrow n' = 4)$ cross section is given in figure 7 and compared to the experimental data of Park *et al* (1976), again renormalized by multiplying by a factor of 0.951. Our results show the same energy dependence as seen experimentally but are somewhat lower, barely reaching the lower edge of the rather large error bars of the experiment. The only previously published coupled channels calculation of $n' = 4$ excitation of which we are aware is the single-centred calculation of Reinhold *et al* (1990). Their coupled channels results for $n' = 4$ excitation are plotted in figure 7. Their results are in close agreement with our calculations and thus are also somewhat low compared to the Park *et al* experiments. An estimate

of the $\sigma(1s \rightarrow n' = 4)$ cross section can be obtained by applying $1/n^3$ scaling to the $\sigma(1s \rightarrow n' = 3)$ cross section. Our calculated $n' = 4$ cross sections are between 11% (at 15 keV) to 18% (at 1 MeV) lower than the $1/n^3$ scaling result. Our cross sections for the individual $\sigma(1s \rightarrow 4l')$ transitions are given in table 6. As the collision energy increases the 4s, 4d and 4f cross sections approach the first Born from above and the 4p cross section approaches first Born from below. The small 4f cross section is somewhat less well converged with respect to the basis than are the other $4l'$ cross sections.

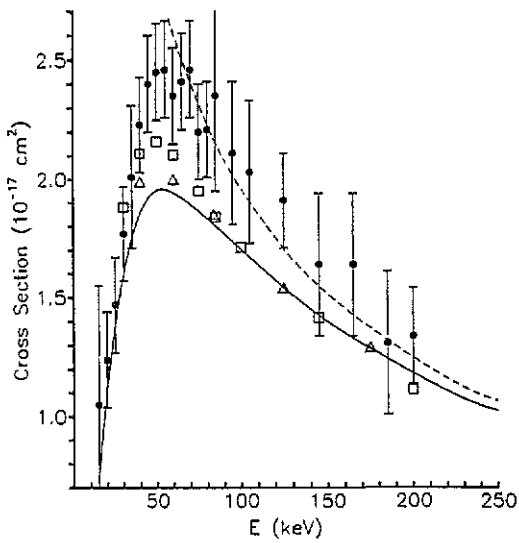

Figure 6. The $1s \rightarrow n' = 3$ excitation cross section. The same notation as in figure 5 is used. In addition, the open squares are the results of the asymmetric two-centred expansion of Ermolaev (1991). The normalization factor applied to the Park *et al* data is the same as in figure 5 and is determined for $n' = 2$; the $n' = 3$ cross sections are not separately normalized. Again note that the vertical scale is linear, so that differences between the various results are readily apparent.

3.2. Electron removal

It is our belief that our single-centred calculations at convergence yield accurate electron removal cross sections even though they do not give the ionization and charge transfer components separately. This supposition is tested in figure 8 where we give our results and compare to experiment. The experimental curve is obtained by adding total capture results ((ORNL 1977) below 220 keV and Hvelplund and Andersen (1982) at the higher energies) to the ionization measurements of Shah and Gilbody (1981) and Shah *et al* (1987). At the low energies the electron removal cross section is dominated by electron capture and at high energies it is dominated by ionization. For example, at 15 keV the experimental cross sections give that capture is 94% of the total whereas at 100 keV ionization is 89% of the total and the capture fraction decreases rapidly at energies above 100 keV. Our results are in good agreement with experiment throughout the entire energy range from 15 keV to 400 keV, where our results have merged with the first Born ionization cross section. This confirms that single-centred calculations pushed to convergence in the angular momenta included in the basis is an accurate procedure for calculating electron removal cross sections, even in situations where the electron capture cross section is large.

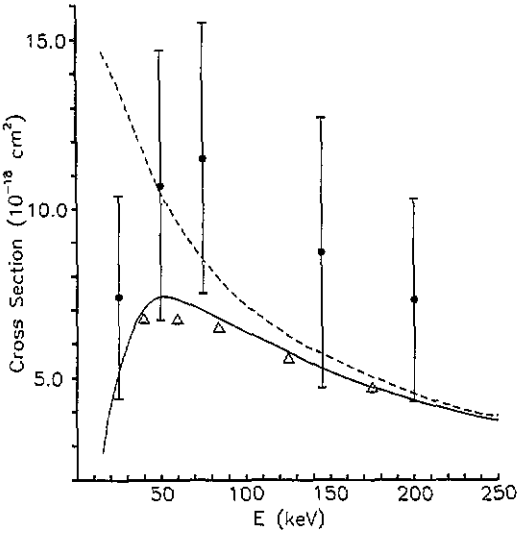

Figure 7. The $1s \rightarrow n' = 4$ excitation cross section. The same notation as in figure 5 is used.

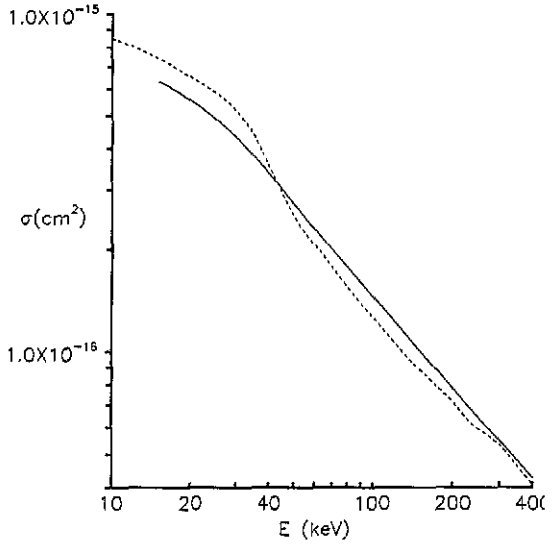

Figure 8. The H(1s) electron removal cross section. The full curve is the present calculation. The broken curve is the sum of the experimental charge transfer (ORNL 1977) and ionization (Shah and Gilbody 1981, Shah *et al* 1987) cross sections.

There have been many other theoretical calculations of capture and ionization and we will not attempt a comprehensive review here. Most other calculations have concentrated on obtaining the separate ionization and capture cross sections rather than the total electron removal. We do note that the extensive triple-centre calculations of Winter and Lin (1984a, b) give at 15 keV, the highest energy at which their results are reported, a capture cross section of 6.3×10^{-16} cm^2 and an ionization cross section of 0.48×10^{-16} cm^2 for a total electron removal cross section of 6.8×10^{-16} cm^2. This is in good agreement with our result of 6.34×10^{-16} cm^2, particularly considering that our convergence errors are largest at this

Table 7. Electron removal cross sections (in units of 10^{-16} cm^2).

E(keV)	Present work	Shakeshaft (1978)	% difference
15	6.34	6.94	+9%
30	4.29	4.0[a]	−7%
45	3.00	2.8[a]	−7%
60	2.29	2.15	−6%
80	1.76	1.7[a]	−3%
100	1.45	1.4[a]	−3%
150	1.01	0.94[a]	−7%
200	0.782	0.66	−16%

[a]Interpolated value.

energy. The previous most extensive calculations of both ionization and total charge transfer in the 15 to 200 keV energy region are the two-centred expansion calculations of Shakeshaft (1978). We compare to his results in table 7. The agreement is quite good. Except at the highest and lowest energies given the two calculations agree to within 7%. We have already discussed our convergence difficulties at 15 keV. At 200 keV the experimental ionization cross section of Shah and Gilbody (1981) is $0.707 \pm 0.021 \times 10^{-16}$ cm^2, midway between the two theoretical results. The very recent two-centred calculations of Toshima (1992) give an ionization cross section of 0.87×10^{-16} cm^2 at 200 keV, well above our result. This calculation is also in qualitative disagreement with ours in regard to the approach of the ionization cross section to the first Born at high collision energies. At 1 MeV our coupled state result for electron removal is virtually identical to the first Born ionization cross section we calculate using our pseudostate basis whereas Toshima gets a cross section 14% larger than the Born at 1 MeV and therefore calls into question the normalization procedure of Shah and Gilbody, who normalized their ionization cross sections to first Born at 1.5 MeV. In Toshima's calculation this difference from the Born at high energies is due to a large contribution (13% at 1.5 MeV) from the high energy ejected electron portion of the projectile-centred continuum. High energy pseudostates are not present in our calculation and the description of high energy projectile-centred states by our target-centred basis would be very difficult. In this regard we note also that our first Born ionization cross sections calculated in our pseudostate basis agrees with an exact PWBA tabulation (Rice *et al* 1977) to within 1.0% up to 60 keV but above this energy our Born results start to fall below and are 4.4% too low at 400 keV and 4.3% too low at 1 MeV. Presumably this is due to an inadequate description in our basis of the high energy portion of the ionization continuum. For all bound–bound transitions and energies considered here our calculated Born cross sections differ at most by 0.5% from exact values, so this small inaccuracy in our Born results at high collision energies is limited to the electron removal cross sections.

4. Summary and conclusions

For p+H(1s) collisions at 15 keV and above we have extended the basis sets used in target-centred coupled states calculations to the point where cross sections converged at the few per cent level are obtained. We believe that the results we have presented establishes the validity of the single-centred basis expansion method for calculating excitation and electron removal cross sections for ion–atom collisions even in situations where charge transfer is large.

Our cross sections are in good agreement with other calculations and with experiment for $n' = 2$ excitation. For $n' = 3$ excitation our results are somewhat below experiment at the cross section peak. Since our cross sections appear converged, especially at these energies of around 40 to 70 keV, the reason for this discrepancy is unclear. For $n' = 4$ excitation the only experiment is that of Park *et al* (1976). The experiment has very large error bars and our results are at their lower edge. Further experimental work for $n' = 3$ and $n' = 4$ excitation, particularly for the individual $n'l'$ components is needed. Our calculations are in quite good agreement with the similar SCE calculations of Reinhold *et al* (1990). We disagree somewhat with the asymmetric two-centred calculations of Ermolaev *et al* (1990a, 1991), substantially so for the individual $3l'$ cross sections. Our calculations as performed here do not distinguish between ionization and charge transfer but give a good accounting of their sum, the electron removal cross section. With the method now established we plan to use it to study other collision systems, particularly those involving excited target initial states.

Acknowledgments

This work was supported by the US National Science Foundation under grant PHY-9009717 and by the Department of Energy under grant DE-FG05-92ER54174. We thank Carlos Reinhold for providing a numerical tabulation of the AO results of Reinhold *et al* 1990.

References

Bransden B H, Dewangan D P and Noble C J 1979 *J. Phys. B: At. Mol. Phys.* **12** 3563–8
Donnelly A, Geddes J and Gilbody H B 1991 *J. Phys. B: At. Mol. Opt. Phys.* **24** 165–72
Ermolaev A M 1990a *J. Phys. B: At. Mol. Opt. Phys.* **23** L45–50
—— 1990b *Phys. Lett.* **149A** 151–4
—— 1991 *J. Phys. B: At. Mol. Opt. Phys.* **24** L495–9
Fitchard E, Ford A L and Reading J F 1977 *Phys. Rev.* A **16** 1325–8
Ford A L, Fitchard E and Reading J F 1977 *Phys. Rev.* A **16** 133–43
Ford A L, Reading J F and Becker R L 1982 *J. Phys. B: At. Mol. Phys.* **15** 3257–73
Fritsch W and Lin C D 1983 *Phys. Rev.* A **27** 3361–4
—— 1991 *Phys. Rep.* **202** 1–97
Hvelplund P and Andersen A 1982 *Phys. Scr.* **26** 375
ORNL 1977 *Oak Ridge National Laboratory Report* No 5206 (unpublished)
Park J T, Aldag J E, George J M and Peacher J L 1976 *Phys. Rev.* A **14** 608–14
Reading J F, Ford A L and Becker R L 1981 *J. Phys. B: At. Mol. Phys.* **14** 1995–2012
—— 1982 *J. Phys. B: At. Mol. Phys.* **15** 625–32
Reinhold C O, Olson R E and Fritsch W 1990 *Phys. Rev.* A **41** 4837–42
Rice R, Basbas G and McDaniel F D 1977 *At. Data Nucl. Data Tables* **20** 503–11
Shah M B, Elliot D S and Gilbody H B 1987 *J. Phys. B: At. Mol. Phys.* **20** 2481–5
Shah M B and Gilbody H B 1981 *J. Phys. B: At. Mol. Phys.* **14** 2361–77
Shakeshaft R 1978 *Phys. Rev.* A **18** 1930–4
Toshima N 1992 *J. Phys. B: At. Mol. Opt. Phys.* **25** L635–40
Winter T G and Lin C D 1984a *Phys. Rev.* A **29** 567–82
—— 1984b *Phys. Rev.* A **29** 3071–7